Long-term influence of giant earthquakes: backward empirical evidence and forward test

Warner Marzocchi, Jacopo Selva

6th December 2007

Istituto Nazionale di Geofisica e Vulcanologia, Sezione di Bologna

Corresponding author: Warner Marzocchi, e-mail: warner.marzocchi@ingv.it

Submitted to: *Bull. Seismol. Soc. Am.*

Abstract

We investigate on the capability of the strongest earthquakes to modify significantly the seismicity in a wide spatio-temporal window. In particular, we show that the strongest earthquakes of last century were probably able to influence the seismicity at large spatio-temporal distances, extending their reach over thousand of kilometers and decades later. We report statistically significant differences between worldwide seismicity before and after the occurrence of such strongest earthquakes of the last century, whose perturbation is modeled by means of co- and post-seismic stress variations. This long-term coupling has produced time variations in the worldwide seismic activity, that appear related to the physical coupling between the focal mechanism of source earthquakes and the tectonic setting of each zone. These results could provide new important insights on seismic hazard assessment, because they raise doubts on the validity of two paradigms, i.e., the steadiness of the mainshock rate, and the isolation of a seismic region compared to the surrounding areas. Finally, beside this backward analysis, we also provide a formal forward test by forecasting the effects on global seismicity of the recent Sumatra-Andaman earthquakes; this is maybe a unique chance to test the long-term hypothesis with an independent dataset that avoids, by definition, any kind of (often unconscious) "optimization" of the results, that is an unavoidable possibility in backward analyses.

1 Introduction

Can a seismic event trigger other earthquakes? Up to a few years ago the answer to this question seemed strictly linked to the dimension of the spatio-temporal scale

considered. Generally speaking, seismic events clustered in space and time are supposed to be connected, as for example in the aftershock sequences, but at large spatio-temporal distances the earthquakes appear to occur independently one from the others, i.e., they are distributed according to a Poisson distribution (Gardner and Knopoff 1974). For a long time, this independence was one of the paradigm in seismology, which had its roots in the apparent lack of a statistically significant correlation between distant (in space and time) earthquakes, and of a plausible physical model for remote triggering. The models based on linear elasticity, for example, which have been successful in explaining a vast range of seismological phenomena, are incapable of accounting for long time lags (i.e., years) in the triggered seismicity and spatial distances beyond few source dimensions of the earthquake rupture. Up to now, the only remarkable empirical evidence in favor of distant (in space) seismic interaction is relative to the dynamical triggering induced by seismic waves. Hill *et al.* (1993) found that the Landers earthquake triggered a remarkably sudden and widespread increase in seismicity at distance up to seventeen source dimensions. Even without statistical tests, the simultaneity of these events is clearly beyond any chance. Since then, the evidence of remote triggering due to dynamical stress interaction increase; among them, we report the case of the Izmit event (Brodsky *et al.*, 2000), and the Denali earthquake (Husen *et al.*, 2004; Prejean *et al.*, 2004). Anyway, despite the large spatial scales involved, the dynamical interaction is not able to explain seismic interaction with time lags greater than minutes/hours.

Even if some researchers already in the sixties and seventies suggested the existence of nonrandom patterns, such as epicenter migrations for large earthquakes (Kagan and Knopoff 1976), only in the last decade the paradigm of independence

among distant (in space and time) seismic events, as well as earthquakes and volcanic eruptions, has been put seriously in doubt (Romanowicz 1993; Pollitz *et al.* 1998; Marzocchi 2002; Casarotti *et al.*, 2001; Melini *et al.*, 2002). The issue had a large impact, but since then controversial arguments fed the long-standing skepticism regarding the feasibility of triggered seismic activity at great spatio-temporal distances. The main doubts are related to the scarce empirical causal evidence (Freed and Lin, 2001; Chéry *et al.*, 2001a, 2001b; Mikumo *et al.*, 2002; Pollitz *et al.*, 2003; Rydelek and Sacks, 2003; Santoyo *et al.*, 2005), and to the fact that the results of recent advances in theoretical modeling of stress diffusion (Stein *et al.* 1992; Pollitz, 1992; Nostro *et al.* 1999) indicate that co- and post-seismic stress perturbations sharply decrease with distance from the epicenter. On the other hand, some researchers suggest that also stress perturbations much less than suspected could be able to trigger an earthquake (see Ziv and Rubin 2000; Rydelek and Sacks 1999, Marzocchi *et al.* 2003).

Here, we look for causal relationship between the occurrence of distant large earthquakes. Specifically, we analyze the worldwide seismicity in order to check if and how giant earthquakes modify the spatio-temporal occurrence of earthquakes, also at large distances and times. Remarkably, the examination consists of a combined theoretical/empirical approach; a suitable physical modeling allows a robust statistical procedure to be applied to the worldwide seismicity, where each event is characterized by both its spatio-temporal occurrence and the stress perturbation due to giant earthquakes.

The use of a combined theoretical/empirical approach makes the analyses more robust, but on the other hand, the strategy requires more assumptions/free-parameters, and the results depend on the reliability of the model used. In order

to account for this, we set the parameters before the tests, independently from the results of the analyses; in this way we avoid any sort of optimization of the results. Nevertheless, we argue that the presence of parameters that are not well constrained could lead to some unknown biases in the results. The only way to avoid any sort of "optimization" of the results is through the analysis of an independent dataset, for instance through a forward analysis. For this reason, we exploit the recent occurrence of two of the most energetic earthquakes of recent times (the Andaman-Sumatra earthquakes) introducing a formal quantitative test to verify their effects on the future seismicity in the surrounding regions.

2 Dataset

We consider a seismic dataset composed by worldwide shallow (depth < 70 km) earthquakes with $M_s \geq 7$ occurred in the time interval 1900-1989 (Pacheco and Sykes 1992; Selva and Marzocchi 2004). The catalog contains the epicentral coordinates, the origin time, the estimates of magnitude and seismic moment, and the estimates of focal mechanism for 621 seismic events. This catalog is a subset of the Pacheco and Sykes' catalog (Pacheco and Sykes 1992) that contains 698 events, because we do not consider the events (77 earthquakes, i.e., the 11% of the total catalog) for which the estimation of the focal mechanism has not been possible (Selva and Marzocchi 2004). Note that the achievement of unbiased results from the following analysis requires the assumption that the stress perturbation induced on the events removed from the catalog are a random sampling of the perturbations related to the whole seismic dataset. Worldwide earthquakes with comparable magnitude are now reported by other catalogs like NEIC and CMT. However, in order to maintain the homogeneity of the dataset, we consider only

the events reported in the Pacheco and Sykes' (1992) catalog that covers a time interval large enough for our purposes.

The catalog is available on the web at *http://www.bo.ingv.it/∼jacopo*. The focal mechanism of the events have been estimated through a statistical procedure that resembles the Kostrov method (Kostrov 1974); the estimates have been found reliable as compared to different solutions available in literature, when available (from CMT after 1977 and few events before). To each mechanism, a reliability label has been assigned, A, B and C for decreasing quality; the analyses of the present work are performed with the largest catalog (A+B+C), but results are checked and found stable even for the smaller (but better constrained) catalogs (A+B and A).

3 Strategy of the analysis

The analysis consists of two steps. In the first step, we model the stress variations induced by five (out of six) of the largest earthquakes in the last century (Kamchatka, 1952; Aleutian Is., 1957; Chile, 1960; Alaska, 1964; Aleutian Is., 1965; see table 1) on the following $M \geq 7.0$ worldwide seismicity. In the second step, we evaluate the statistical significance of the variations of the earthquakes spatio-temporal distribution accounting for stress perturbations. The choice to consider only the largest five (only Kanto earthquake occurred in 1923 has a comparable seismic energy released) earthquakes as possible "sources" of global changes in seismicity requires further explanation. This choice is mainly driven by a practical advantage; the time clustering of such events on the middle of the catalog allows us to clearly separate a part of the catalog "before" and one "after" such events. From a physical point of view, it is reasonable to suppose that a lower threshold for

remote triggering does not exist, and that the larger the stress induced, the more significant the change in probability of a seismic event. In this perspective, our selection implicitly assumes that the effects of the five largest events of the past century are, on average, predominant over the local perturbations due to smaller events.

3.1 Modeling the stress perturbations

Stress perturbations are evaluated in terms of variation of Coulomb Failure Function (CFF), ν (in KPa), and of CFF rate variation, $\dot{\nu}$ (in KPa yr^{-1}), by means of a spherical, viscoelastic, stratified and self-gravitating Earth model (Piersanti *et al.* 1995). In brief, the model is 1-D for rheology and 3-D for geometry.

In particular, we use the model proposed by Piersanti *et al.* (1995) with these parameters: Core radius = 3471 Km; mantle thickness = 2620 Km; mantle Maxwell viscosity = 10^{21} Pa s; asthenosphere thickness = 200 Km; asthenosphere Maxwell viscosity = $1 \cdot 10^{18}$, $5 \cdot 10^{18}$ (figures and tables 2 and 3 report the results obtained with this viscosity), $1 \cdot 10^{19}$, $5 \cdot 10^{19}$, and $1 \cdot 10^{20}$ Pa s; lithosphere thickness = 80 Km. The choice of the asthenosphere viscosity deserves more explanation. Previous studies have suggested that the evolution of the stress perturbation might be better modeled with a non-linear readjustment of the asthenosphere (Giunchi and Spada 2000; Pollitz *et al.* 2001). This non-linearity may be modeled by varying the viscosity of the asthenosphere as a function of the time lag from the earthquake. Just after an earthquake, the time behavior of the stress perturbation seems to be in agreement with values of the viscosity even smaller than 10^{18} Pa s, so that the effective perturbation might evolve quicker than how it does in our Earth model; on the other hand, for longer time lags, viscosity up to 10^{20} Pa s have

been estimated (e.g., Piersanti 1999). It is worth noting that the model has been designed to work at global scale, therefore it neglects the details of the seismogenic fault (considered as a source segment), that are important in the proximity of the faults. Along the same line, the model considers self-gravitation and neglects the compressibility, because at a global scale the former is more important than the latter.

As regards the evaluation of the stress perturbations, we calculate ν through equation

$$\nu = \sigma_\tau + \mu' \sigma_n$$

where σ_τ is the shear stress on the fault, σ_n is the normal stress that clumps the fault, and μ' is the apparent friction coefficient (King and Cocco 2001). The parameter μ' includes the effects of fluids on the fault, and its value ranges in the interval $[0, 0.75]$ (Cocco and Rice 2002). Low values are typical for "undrained" conditions (Deng and Sykes 1997), i.e., for time intervals of weeks/few months that are relevant for studying aftershocks sequences. On the other hand, high values are typical of "drained" condition, i.e., for times much larger than months (Deng and Sykes 1997). For this reason we use $\mu' = 0.75$ (figures and tables 2 and 3 report the results obtained with this value) and 0.60. For what concerns $\dot{\nu}$, we calculate it as

$$\dot{\nu}(t) = [\nu(t) - \nu(t - 1\text{yr})]/1\text{yr} \qquad .$$

In other words, $\dot{\nu}$ represents the numerical evaluation of the temporal derivative of ν filtered over a time scale of one year, because post-seismic variations have characteristic times $\gg 1$ year (Selva and Marzocchi 2005).

Compared to more traditional approaches where only ν is considered (Stein *et al.* 1992), we also look at $\dot{\nu}$, because it may be more effective to study the long-

term coupling among earthquakes, since it can increase or decrease the tectonic stress loading rate (Marzocchi *et al.* 2003; Selva and Marzocchi 2005), that is ultimately strictly related to the seismic activity.

Perturbations in terms of ν and $\dot{\nu}$ are modeled for all the events occurring after the giant earthquakes. Since ν and $\dot{\nu}$ do not follow any a priori known statistical distribution, in order to have a "reference" distribution for the unperturbed case, we model also the stress variations (ν and $\dot{\nu}$) that the five source events would have induced on the earthquakes that occurred before (that are obviously not perturbed by them) as if they had occurred after them. Therefore, the dataset consists of 176 earthquakes occurred in the time period I that spans from 1928-1951 (ν_I and $\dot{\nu}_I$), and of 173 earthquakes occurred in the time period II that ranges from 1966 to 1989 (ν_{II} and $\dot{\nu}_{II}$). The two time intervals have the same length, and are before and after the giant earthquakes that occurred all between 1952 and 1965 (see table 1). Since the time between source and receiving earthquakes has to be positive in the model, at each event occurred in period I is attributed a fictitious time $t^\star = t_i + T_0$, where t_i is the real time of occurrence of the i-th earthquake and T_0 is the time interval between 1/1/1928 and 1/1/1966; in other words, the time of occurrence of all the earthquakes of period I is shifted forward 38 years. We do not consider the events in the period 1900-1927 because they could be affected by giant earthquakes occurred at the end of the previous century and therefore not reported by the catalog. In figure 1, we report the seismic moment of all events reported in the catalog. From the figure we can see that the period 1952-1965 contains 5 out of 6 the largest events of the century. In the reference period I only the Kanto earthquake occurred in 1923 has a magnitude comparable to the Aleutine earthquakes of 1957 and 1965, but it is an order of magnitude less than the seismic

moment of Alaska 1964 and Chile (1960) events. Our analysis assumes that the effects at a global scale of the Kanto earthquake alone is negligible compared to the perturbations produced by the five events considered. Obviously, this does not preclude the possibility that the Kanto event may have created a local important perturbation on surrounding seismicity.

3.2 Testing the variations of earthquakes distribution

In the second step, we check if ν and $\dot{\nu}$ calculated in the periods I and II are significantly different. The main rationale of the comparison is that if giant earthquakes have a statistically significant influence on the occurrence of the worldwide earthquakes, we should find a statistical difference between ν and/or $\dot{\nu}$ calculated in period I and II, i.e., before and after the occurrence of such source earthquakes. In particular, we check the influence of giant earthquakes by means of three statistical tests relative to three different null hypotheses. The use of different tests allows to check the stability of the results as a function of the particular null hypothesis under test. The first null hypothesis ($H_0^{(1)}$) is that the probability to have positive values of the variable considered (ν and $\dot{\nu}$) for time periods I and II is equal to 0.5, i.e., negative and positive values have the same probability; we use a binomial test to calculate the significance level at which we can reject $H_0^{(1)}$. The second null hypothesis ($H_0^{(2)}$) is that the median of the variable considered (ν and $\dot{\nu}$) for time periods I and II are not larger than zero (one tail test); we use a Wilcoxon signed-rank test (Gibbons 1971) to calculate the significance level at which we can reject $H_0^{(2)}$. The third null hypothesis ($H_0^{(3)}$) is that the median of ν and $\dot{\nu}$ calculated in period II is not larger than the median calculated for period I (one tail test); in this case we use the classic Wilcoxon test (Gibbons 1971) to

calculate the significance level at which we reject $H_0^{(3)}$.

It is worth remarking the role of "reference" distribution of perturbations defined for period I. For the hypothesis $H_0^{(3)}$, there is a direct comparison between period I and II so that we expect distributions to be different if giant earthquakes do affect subsequent events. For the hypotheses $H_0^{(1)}$ and $H_0^{(2)}$, instead, periods I and II are considered separately; the tests for period I aim basically to identify possible "geometric" biases introduced by the fact that earthquakes can occur in locations characterized prevalently by positive (or negative) ν and/or $\dot{\nu}$ by pure chance, i.e., without any link with perturbations. Since earthquakes of period I have not been influenced by the giant earthquakes perturbation given that they occurred before, the rejection of $H_0^{(1)}$ and/or $H_0^{(2)}$ for this period would imply that such events are somehow overall coupled, not depending on a specific influence of giant earthquakes. It follows that the results of these two tests for period I are fundamental "reference" tests to interpret correctly the meaning of the same tests for period II.

In order to explain the physical implications of the three tests, we discuss in advance two hypothetical expected results of the tests for the two end cases where giant earthquakes have - and do not have - a significant influence on the subsequent seismicity.

- *Case 1: giant earthquakes do not affect the following seismicity.* We expect that the tests for $H_0^{(1)}$ and $H_0^{(2)}$ have equivalent results for periods I and II, and that $H_0^{(3)}$ is not rejected. In this case there would not be any reason to see differences in these two periods of time, before and after the occurrence of giant earthquakes.

- *Case 2: giant earthquakes affect the following seismicity (through long-term*

interaction), and there is no geometric biases into the epicenter locations. We expect $H_0^{(1)}$ and $H_0^{(2)}$ to be rejected for period II and to be not rejected for period I, and $H_0^{(3)}$ to be rejected. In this case the distribution of ν and/or $\dot{\nu}$ is different for the two periods of time, before and after the giant earthquakes, and perturbations favor most the events in period II.

4 Results of the analysis and stability check

The results of the tests are reported in tables 2 (results of $H_0^{(1)}$ and $H_0^{(2)}$), and 3 (results of $H_0^{(3)}$), and in figure 2. All results are relative to an Earth model with viscosity of the asthenosphere equal to $5 \cdot 10^{18}$ Pa s, and $\mu' = 0.75$.

The tests of the hypotheses of $H_0^{(1)}$ and $H_0^{(2)}$ (Table 2) for period I show that the distribution of positive and negative values of $\dot{\nu}_I$ are the same, implying the lack of a geometrical bias; at the same time, we reject both hypotheses (with a significance level lesser than 0.01) for $\dot{\nu}_{II}$, indicating a prevalence of positive values of induced stress rates after the giant earthquakes. As regards the hypothesis $H_0^{(3)}$, the central value of the distribution of $\dot{\nu}_{II}$ is significantly larger (significance level of 0.02) than the corresponding value of $\dot{\nu}_I$. In summary, earthquakes occurred in period II are characterized by more positive and larger values of $\dot{\nu}$ than the events occurred in period I. The results for ν, instead, do not show any significant difference before and after giant earthquakes.

We verify the stability of the results by using different viscosities ($1 \cdot 10^{18}, 5 \cdot 10^{18}, 1 \cdot 10^{19}, 5 \cdot 10^{19}$ and $1 \cdot 10^{20}$ Pa s), different values of the apparent friction coefficient μ' ($\mu' = 0.75$ and 0.6), and subsets of the seismic catalog where the focal mechanisms are better constrained (earthquakes with selection flag A and B in Selva and Marzocchi, 2004). The stability results for $\dot{\nu}$ show that the values of

period II are always larger than the ones relative to period I. In some cases (for instance, with $\mu' = 0.6$, and with subsets of better constrained focal mechanisms), the statistical evidence are more statistically significant than the once shown in tables 2 and 3. Conversely, the stability results for ν show a strong dependence on the viscosity, and no stable results are evident.

To summarize, we find a significant difference (significance level less than 0.02) between $\dot{\nu}$ of period I and II; in particular, the rates observed for period II are more positive than for the previous period. This difference cannot be explained by some sort of bias in epicenter location.

5 Discussion of the results

The results reported above stand for a significant perturbation (significance levels lesser than 0.02) of the giant earthquakes on the worldwide seismicity. The perturbation consists of variation of $\dot{\nu}$ that increases (or decreases) the tectonic loading of a seismogenic fault, also far from the source. Remarkably, we do not find any stable difference in ν values, implying that the stress induced may not be the most relevant parameter in promoting changes in seismicity, at least over a large time-distance domain. An alternative interpretation of our results is that if ν is a relevant factor for long-term seismic interaction, we need a much more detailed model (for instance, in terms of better constrained viscosity of the asthenosphere, and friction process modeling) to verify this hypothesis.

Remarkably, the influence of giant earthquakes can explain worldwide time variations of seismicity rate over time intervals of decades (Kagan and Jackson, 1991; Marzocchi *et al.*, 2003; Selva and Marzocchi, 2005; Lombardi and Marzocchi,

2007). At this purpose, in figure 3, we report a plot of the variable Δ defined as

$$\Delta = (N_{II}^{(+)} - N_{I}^{(+)}) + (N_{I}^{(-)} - N_{II}^{(-)})$$

where $N_{I}^{(+)}$ and $N_{II}^{(+)}$ are the number of earthquakes with positive $\dot{\nu}$ in the period I and II, respectively, and $N_{I}^{(-)}$ and $N_{II}^{(-)}$ are the number of earthquakes with negative $\dot{\nu}$ in the period I and II, respectively. The events are taken inside a circle with a radius of 1000 km and centered at the nodes of a grid $1^\circ \times 1^\circ$. In few words, positive/negative values of Δ represent a variation of the rate of occurrence in accordance/opposition with $\dot{\nu}$. The figure shows that the variation of the rate of occurrence of the worldwide seismicity is almost everywhere in agreement with the sign of $\dot{\nu}$. The only relevant exception is for Alaska. This area experienced a decrease of the rate of occurrence of large earthquakes after the sixties, even though the source earthquakes induced a $\dot{\nu}$ that is in accordance with regional tectonics (in fact, the source earthquakes would have induced positive values on events occurred in period I). We interpret this discrepancy with the fact that the very large seismic activity in this region in the sixties (and even before) could have unloaded almost all the seismogenic structures able to produce large events; note, for example, that the negative anomaly of Δ is mainly located on the fault area of the 1964 event.

Another important feature is that the most perturbed areas do not have a specific spatial pattern, for instance, they are not the closest to the source earthquakes. This means that the sign of the stress perturbation may be more important than its amplitude. This could be due to the fact that the local stress state before the perturbation is one main factor in remote triggering; in other words, it is necessary that the stress state of one seismic region is close to a critical state in order to be sensitive to remote stress perturbations. This thought implies that the amplitude

of the stress is not the only ingredient to be considered to investigate on seismic trigger; also the spatial coverage may be important, because a larger area means a higher probability to find regions close to a critical state. In this respect, it is worth noting that the post-seismic effects of giant earthquakes could be more effective than co-seismic effects to affect global seismicity because they have a smoother spatial decay, i.e., a larger spatial coverage. Notably, this conjecture can also explain the evidence of remote dynamical triggering that do not appear to have, similarly to the present case, any spatial pattern.

In spite of the agreement in the overall trend, other aspects deserve more investigation. The most important is related to the amplitude of the post-seismic stress perturbations (see values in table 2). At first, note that the energy of giant earthquakes, as clearly seen after the Sumatra-Andaman Islands 2004 event, is probably severely underestimated (Lay *et al.* 2005) by classical source estimation procedures, due to the significant slow slip that affects periods longer than the ones recorded from classical seismometers. Moreover, other effects, such as the post-slip on the co-seismic slip area, or at deeper depths, may significantly increase the final slip and area of the dislocation, so that the actual energy released (source of the stress perturbation field) may be significantly higher than what usually modeled for such events.

Neglecting all these possible biases introduced by our calculations, the stress rate induced by the source earthquakes may be three orders of magnitude less than, for example, the tectonic rate in southern California. A deep discussion of this issue is reported in Marzocchi *et al.* (2003) and Selva and Marzocchi (2005). Here, we just want to remark that $\dot{\nu}$ acts over a surprisingly stable tectonic motion, that shows comparable velocities over time intervals which span 5 order of magnitude,

i.e., from few years up to millions of years (Sella *et al.* 2002; DeMets *et al.* 1994). We remark that this stability is far from obvious, since it implies the presence of very low non-seismic fluctuations of the tectonic motion, and maybe of the mean regional tectonic rate. In this case, also "apparently small" post-seismic stress rates may influence significantly the tectonic rates. It is also worth noting that the same point may be valid also for static stress changes, where it has been proposed that perturbations as large as tenth of bars may reasonably promote earthquakes (Reasemberg and Simpson 1992), at depth where the lithostatic pressure is also four orders of magnitude greater than such a proposed threshold.

For what concerns more practical aspects, the presence of a systematic behavior in the data could have a significant impact in seismic hazard assessment, improving earthquake forecasting. In particular, the results obtained arise doubts on the validity of two paradigms of seismic hazard assessment, i.e., the steadiness of the mainshock rate, and the isolation of a seismic region compared to the surrounding areas.

6 A forward test: forecasting the long-term effects of the Sumatra-Andaman 2004-2005 earthquakes

The intrinsic nature of backward analyses does not allow to rule out the possibility that the results reported above are due to some sort of unconscious "retrospective realism". In other words, the impossibility to set the model of interaction and the null hypotheses of the statistical test independently from the observations available leads to the possibility that the results obtained in a backward analysis may be

always potentially biased towards conscious or unconscious a priori convictions. In practice, backward analyses represent almost always a necessary but not sufficient evidence to prove some a priori hypothesis. For this reason, we report a forward analysis relative to the effects of the recent Andaman-Sumatra giant earthquakes. We think that this is the only way to evaluate in a convincing way, the long-term interaction hypothesis.

Specifically, we report in figure 4 the effects on the worldwide seismicity of the recent Sumatra-Andaman earthquakes (focal mechanism as in Lay *et al.* 2005). We first subdivide the Earth surface by using the Flinn-Engdahl's regionalization scheme (Flinn *et al.* 1974; Young *et al.* 1996), and then we calculate the two conjugate average focal mechanisms for each cell by means of the Kostrov's method (Kostrov 1974) with the events reported in the CMT catalog (Dziewonski *et al.*, 1981; Dziewonski and Woodhouse 1983). In the calculation we keep only the zones that have i) a low dispersion of the focal mechanisms around the average that stands for almost homogeneous tectonic areas ($\eta < 0.2$; η is defined in Nettles and Ekstrom (1998)), ii) at least one earthquake with $M \geq 6.0$, and iii) a spatial distance less than 10,000 kilometers from the sources.

For each of these average focal mechanisms we calculate $\dot{\nu}$ induced by the Sumatra-Andaman earthquakes, reporting positive (in accordance with regional tectonics) and negative (in opposition to regional tectonics) values (see table 4 and figure 4). In table 4, we report label and name of each region and the sign of $\dot{\nu}$ induced by the Sumatra-Andaman earthquakes both on the "preferred" and the conjugate plane. Note that we report the sign of $\dot{\nu}$ rather than its amplitude, because of the results reported in figure 3 and discussed above. Since the choice of the most realistic focal mechanism among the two is not always straightforward, in

figure 4 we report the solution for the "preferred" focal mechanism, for its conjugate, and the areas where the sign is stable for the two solutions. The "preferred" focal mechanism solution is chosen by selecting the fault with the lowest dip angle for both rakes in the interval $[65°, 115°]$ (thrust events), and the fault with the highest dip angle otherwise. We are aware that this is only a first approximation, but our purpose here is to provide a general scheme of the global seismic changes induced by the recent giant Sumatra-Andaman earthquakes.

This map and table 4 are the basis to build a quantitative forward test for the long-term seismic coupling. In general, if the long-term seismic coupling is a real effect, zones colored in red (i.e., $\dot{\nu}$ in accordance with regional tectonics) have a larger propensity to experience an increase of earthquakes occurrence in the next years/few decades. On the contrary, zones colored in blue (i.e., $\dot{\nu}$ in opposition to regional tectonics) have a larger propensity to experience a decrease of earthquakes occurrence in the same interval of time ad above. For the forward test, the null hypothesis to be tested is $\pi_1 = \pi_2$, where π_1 is the proportion of earthquakes with M_s7.0+ occurred in red areas before the Andaman-Sumatra earthquakes, and π_2 is the same quantity calculated for the earthquakes occurred in the red areas after the Andaman-Sumatra earthquakes. In practice, the forward test can be schematized in 4 steps:

1. To select a time interval of equal length τ, before and after the Andaman-Sumatra earthquakes. The value of τ depends on the time history of the stress perturbation that can last decades, and it does not have to overlap effects of previous giant earthquakes. Taking into account both requirements, we set $\tau = 15$ years. For this value we have the largest effects in terms of stress rate induced, and we avoid the overlap with the effects of the giant

earthquakes occurred in the sixties.

2. To count the number of earthquakes with M_s7.0+ occurred in the red ($M_r^{(\cdot)}$) and blue ($M_b^{(\cdot)}$) areas with coherent focal mechanisms (see the map at the bottom of figure 4) before ($M_r^{(1)}$, $M_b^{(1)}$) and after ($M_r^{(2)}$, $M_b^{(2)}$) the Andaman-Sumatra earthquakes, and to estimate the sampling proportion $\hat{\pi}_1 = M_r^{(1)}/(M_r^{(1)} + M_b^{(1)})$, and $\hat{\pi}_2 = M_r^{(2)}/(M_r^{(2)} + M_b^{(2)})$.

3. To calculate the statistic

$$z = \frac{(\hat{\pi}_1 - \hat{\pi}_2)}{\sqrt{P(1-P)[1/(M_r^{(1)} + M_b^{(1)}) + 1/(M_r^{(2)} + M_b^{(2)})]}} \tag{1}$$

where

$$P = \frac{\hat{\pi}_1(M_r^{(1)} + M_b^{(1)}) + \hat{\pi}_2(M_r^{(2)} + M_b^{(2)})}{(M_r^{(1)} + M_b^{(1)}) + (M_r^{(1)} + M_b^{(1)})} \tag{2}$$

The statistic z can be considered normally distributed for $(M_r^{(1)} + M_b^{(1)})$ and $(M_r^{(2)} + M_b^{(2)})$ larger than ten.

4. To evaluate the significance level at which the null hypothesis can be rejected.

We select only earthquakes with M$_s$7.0+ for the sake of homogeneity with backward analyses, and because the rate of M$_s$7.0+ earthquakes is a good proxy for the "background" seismic activity, being almost all "mainshocks". In fact, catalogs of smaller earthquakes are dominated by aftershocks, and their removal is always a delicate issue that can introduce some sort of "control" on the results of the forward test.

Note that this forward test also evaluates the forecasting capability of the remote triggering. However, it is worth remarking that the null hypothesis rejection of this forward test is a sufficient, but not necessary condition to check the feasibility of remote triggering. In fact, in the backward analysis we note that the stress

perturbations of giant earthquakes do not only modify the earthquake rate, but tend to also modify the prevalent focal mechanism of a region (see, for example, the Chilean area in figure 2, and Selva and Marzocchi 2005). This hypothesis can be only tested a posteriori, by using the same tests adopted here; in this case, the independence of the check of this retrospective analysis is granted by using the same parameters and tests adopted here.

7 Final remarks

The purpose of this paper is to evaluate the capability of the strongest earthquakes to modify the seismicity in large space-time windows. For this purpose, we have analyzed the catalog of the worldwide shallow earthquake of the last century with M_s 7.0+. A backward analysis has shown a statistically significant difference between the spatio-temporal distribution of earthquakes occurred before and after the sixties (when the strongest earthquakes occurred) if we account for stress rate perturbations induced by giant earthquakes; remarkably, stress rates seem to be more important than stress values. Finally, in order to avoid any possible biases intrinsically linked to any backward analysis, we have also provided clear quantitative rules that can be used in the future to evaluate the remote triggering hypothesis with a completely independent dataset.

Acknowledgements: The authors thank the Associate Editor (C. Trifu), and the reviewers (B. Romanowicz and T. Lay) for their helpful comments that improve the quality of the manuscript.

Bibliography

Ben-Menahem A. and Toksoz, M.N., 1963. Source Mechanism from Spectrums of Long-Period Surface Waves. 2. The Kamchatka Earthquake of November 4, 1952, *J. Geophys. Res.*, **68**, No. 18, 5207-5222.

Brodsky, E. E., V. Karakostas, and H. Kanamori, 2000. A new observation of dynamically triggered regional seismicity: earthquakes in Greece following the August 1999 Izmit, Turkey Earthquake. *Geophys. Res. Lett.*, **27**, 27412744.

Casarotti, E., A. Piersanti, F. P. Lucente, E. Boschi, 2001. Global postseismic stress diffusion and fault interaction at long distances. *Earth Plan. Sci. Lett.*, **191**, 75-84.

Chéry J., Merkel S., Bouissou, S., 2001a. A Physical Basis for Time Clustering of Large Earthquakes, *Bull. Seism. Soc. Am.*, **91**, 1685-1693.

Chéry J., Carretier S., Ritz, J.F., 2001b. Postseismic stress transfer explains time clustering of large earthquakes in Mongolia, *Earth Planet. Sci. Lett.*, **194**, 277-286.

Cocco, M. and Rice, J.R., 2002. Pore pressure and poroelasticity effects in Coulomb stress analysis of earthquake interactions, *J. Geophys. Res.*, **107(B2)**, 10.1029/2000JB000138, pp. ESE.2.1 - ESE.2.17.

DeMets, S., Fordon, R.G., Argus, D.F. and Stein, S., 1994. Effect of recent revisions to the geomagnetic reversal time scale on estimates of current plate motions, *Geophys. Res. Lett.*, **21**, No. 20, 2191-2194.

Deng, J. and Sykes, L.R., 1997. Stress evolution in southern California and triggering of moderate-, small-, and micro-size earthquakes, *J. Geophys. Res.*, **102**, B11, 24,411-24,435.

Dziewonski, A. M., Chou, T. A., and Woodhouse, J. H., 1981. Determination of earthquake source parameters from waveform data for studies of global and regional seismicity. *J. Geophys. Res.*, **86**, 2825 2852.

Dziewonski, A. M. and Woodhouse, J. H., 1983. An experiment in systematic study of global seismicity: Centroid-moment tensor solutions for 201 moderate and large earthquakes of 1981, *J. Geophys. Res.*, **88**, 3247 3271.

Flinn, E. A., Engdahl, E. R. and Hill, A. R., 1974. Seismic and Geographical Regionalization, *Bull. Seismol. Soc. Am.*, **64**, 771 992.

Freed A.M. and Lin J., 2001. Delayed triggering of the 1999 Hector Mine earthquake by viscoelastic stress transfer. *Nature*, **411**, 180-183.

Gardner, J. and Knopoff, L., 1974. Is the sequence of earthquakes in southern California with aftershocks removed Poissonian? Yes, *Bull. Seismol. Soc. Amer.*, **64**, 1363-1367.

Gibbons, J.D., 1971. *Non–parametric Statistical Inference*, McGraw–Hill, New York, 306 pp.

Giunchi, C. and Spada, G., 2000. Postglacial rebound in a non-Newtonian spherical Earth, *Geophys. Res. Lett.*, **27(14)**, 2065-2068, DOI: 10.1029/2000GL011460.

Hill, D.P., *et al.*, 1993. Seismicity remotely triggered by the magnitude 7.3

Landers, California, earthquake, *Science*, **260**, 1617-1623.

Husen, S., R. Taylor, R. B. Smith, and H. Healser, 2004. Changes in geyser eruption behavior and remotely triggered seismicity in Yellowstone National Park produced by the 2002 M 7.9 Denali Fault earthquake, Alaska. *Geology*, **32**, 537540.

Johnson, J.M., Tanioka, Y., Ruff, L.J., Satake, K., Kanamori, H. and Sykes, L.R., 1994. The 1957 great Aleutian earthquake, *Pure Appl. Geophys.*, **142**, No 1, 3-28, DOI: 10.1007/BF00875966.

Kagan, Y. and Knopoff, L., 1976. Statistical search for non-random features of the seismicity of strong earthquakes, *Phys. Earth Planet. Int.*, **12**, 291-318.

Kagan Y.Y. and Jackson, D.D., 1991. Long-term earthquake clustering, *Geophys. J. Int.*, **104**, 117-133.

Kanamori, H. and Cipar, J.J., 1974. Focal processes of the Great Chilean earthquake of May 22, 1960, *Phys. Earth Planet. Int.*, **9**, 128-136.

Kanamori, H., 1970. The Alaska earthquake of 1964: Radiation of long-period surface waves and source mechanism, *J. Geophys Res.*, **75**, 5029-5040.

Kanamori, H., 1977. The energy release in great earthquakes, *J. Geophys. Res.*, **82**, 2981-2987.

King, G.C.P. and Cocco, M., 2001. Fault interaction by elastic stress changes: New clues from earthquake sequences, *Adv. Geophys.*, **44**, 1-38.

Kostrov, V. V., 1974. Seismic moment and energy of earthquakes, and seismic

flow of rock, *Izv. Acad. Sci. USSR, Phys. Solid Earth*, Engl. Trans., 1, 23 44.

Lay, T. *et al.*, 2005. The Great Sumatra-Andaman Earthquake of 26 December 2004, *Science*, **308**, no. 5725, 1127-1133, DOI: 10.1126/science.1112250.

Lombardi A.M., and W. Marzocchi, 2007. Evidence of clustering and nonstationarity in the time distribution of large worldwide earthquakes, *J. Geophys. Res.*, **112**, B02303, doi:10.1029/2006JB004568.

Marzocchi, W., 2002. Remote seismic influence on large explosive eruptions, *J. Geophys. Res.*, **107(B1)**, doi:10.1029/2001JB000307.

Marzocchi, W., Selva, J., Piersanti, A. and Boschi, E., 2003. On the long-term interaction among earthquakes: Some insight from a model simulation, *J. Geophys. Res.*, **108**, B11, 2538, doi:10.1029/2003JB002390.

Melini, D., E. Casarotti, A. Piersanti, 2002. New insights on long distance fault interaction. *Earth Plan. Sci. Lett.*, **204**, 363-372.

Mikumo T., Yagi Y., Singh S.K., Santoyo M.A., 2002. Coseismic and postseismic stress changes in subducting plate: possible stress interactions between large interplate thrust and intraplate normal-faulting earthquakes. *J. Geophys. Res.*, **107**, doi:10.1029/2001JB000446.

Nettles, M. and Ekström, G., 1998. Faulting mechanism of anomalous earthquakes near Brdarbunga Volcano, Iceland, *J. Geophys. Res.* **103(B8)**, 17973-17984, 10.1029/98JB01392.

Nostro, C., A. Piersanti, A. Antonioli, G. Spada, 1999. Spherical versus flat models

of coseismic and postseismic deformations. *J. Geophys. Res.*, **104** 13,115- 13,134.

Pacheco, J.F. and Sykes, L.R., 1992. Seismic moment catalog of large shallow earthquakes, 1900 to 1989, *Bull. Seismol. Soc. Am.*, **82**, 1306-1349.

Piersanti, A., 1999. Postseismic deformation in Chile: Constraints on the asthenospheric viscosity, *Geophys. Res. Lett., 26(20)*, 3157-3160, 10.1029/1999GL005375, 1999.

Piersanti, A., Spada, G., Sabadini, R. and Bonafede, M., 1995. Global postseismic deformation, *Geophys. J. Int.*, **120**, 544-566.

Pollitz, F.F., 1992. Postseismic relaxation theory on the spherical Earth, *Bull. Seismol. Soc. Am.*, **82**, 422-453.

Pollitz, F.F., Bürgmann, R. and Romanowicz, B., 1998. Viscosity of oceanic asthenosphere inferred from remote triggering of earthquakes, *Science*, **280**, 1245-1249.

Pollitz, F.F., Wicks, C. and Thatcher, W., 2001. Mantle Flow Beneath a Continental Strike-Slip Fault: Postseismic Deformation After the 1999 Hector Mine Earthquake, *Science*, **293**, 1814-1818.

Pollitz F.F., Vergnolle M., Calais E., 2003. Fault interaction and stress triggering of twentieth century earthquakes in Mongolia. *J. Geophys. Res.*, **108**, 2503, doi:10.1029/2002JB002375.

Prejean, K., D. P. Hill, E. E. Brodsky, S. E. Hough, M. J. S. Johnston, S. D. Malone, D. H. Oppenheimer, A. M. Pitt, and K. B. Richards-Dinger, 2004.

Remotely triggered seismicity on the United States west coast following the Mw 7.9 Denali Fault earthquake. *Bull. Seism. Soc. Am.*, **94**, S348S359.

Reasenberg, P.A. and Simpson, R.W., 1992. Response of Regional Seismicity to the Static Stress Change Produced by the Loma Prieta Earthquake, *Science*, **255**, 1687-1690.

Romanowicz, B., 1993. Spatiotemporal patterns in the energy release of great earthquakes, *Science*, **260**, 1923-1926.

Rydelek, P. A., and Sacks,I. S., 1999. Large earthquake occurrence affected by small stress changes, *Bull. Seismol. Soc. Am.*, **89**, 822 828.

Rydelek P.A., and Sacks I.S., 2003. Triggering and inhibition of great Japanese earthquakes: the effect of Nobi 1891 on Tonakai 1944, Nankaido 1946 and Tokai. *Earth Plan. Sci. Lett.*, **206**, 289-296.

Santoyo M.A., Singh S.K., Mikumo T., Ordaz M., 2005. Space-time clustering of large thrust earthquakes along the mexican subduction zone: an evidence of source stress interaction. *Bull. Seism. Soc. Am.*, **95**, 1856-1864, doi:10.1785/0120040185.

Sella, G.F., Dixon, T.H. and Mao, A., 2002. REVEL: A model for Recent plate velocities from space geodesy, *J. Geophys. Res.*, **107**, No. B4, 10.1029/2000JB000033.

Selva, J. and Marzocchi, W., 2004. Focal parameters, depth estimation, and plane selection of the worldwide shallow seismicity with $M_s \geq 7.0$ for the period 1900-1976, *Geochem. Geophys. Geosyst.* **5**, Q05005, doi:10.1029/2003GC000669.

Selva J. and Marzocchi, W., 2005. Variations of southern California seismicity:

Empirical evidence and possible physical causes, *J. Geophys. Res.*, **110**, B11306, doi:10.1029/2004JB003494.

Stein, R.S., King, G.C.P. and Lin, J., 1992. Change in failure stress on the southern San Andreas fault system caused by the 1992 magnitude = 7.4 Landers earthquake, *Science*, **258**, 1328-1332.

Young, J.B., Presgrave, B.W., Aichele, H., Wiens, D.A. and Flinn, E.A., 1996. The Flinn-Engdahl Regionalisation Scheme: The 1995 Revision, *Phys. Earth Plan. Int.*, **96**, 223-297.

Ziv, A., and Rubin, A. M., 2000. Static stress transfer and earthquake triggering: No lower threshold in sight?, *J. Geophys. Res.*, **105**, 13,631 13,642.

Earthquake	Reference
Kamchatka, 1952	Ben-Menahem and Toksoz 1963
Aleutinian Is., 1957	Johnson *et al.* 1994
Chile, 1960	Kanamori and Cipar 1974
Alaska, 1964	Kanamori 1970
Aleutinian Is., 1965	Kanamori 1977

Table 1: References for the focal mechanisms of source earthquakes.

Dataset	N	N_+	p_{10}	p_{50}	p_{90}	$\alpha^{(1)}$	$\alpha^{(2)}$
ν_I [KPa]	176	94	-0.89	0.014	2.5	0.18	0.72
ν_{II} [KPa]	173	100	-0.72	0.020	1.2	0.02	0.23
$\dot{\nu}_I$ [KPa yr^{-1}]	176	93	-0.026	$1.6 \cdot 10^{-3}$	0.153	0.22	0.51
$\dot{\nu}_{\mathbf{II}}$ [KPa yr^{-1}]	**173**	**116**	**-0.025**	$\mathbf{2.7 \cdot 10^{-3}}$	**0.065**	**<0.01**	**<0.01**

Table 2: Results of the test of hypotheses $H_0^{(1)}$ and $H_0^{(2)}$. The first column reports the dataset used, the second the total number of data (N), the third the number of positive values (N_+), the fourth, fifth, and sixth, the 10th, 50th (median), and 90th percentiles, the seventh the significance level ($\alpha^{(1)}$) of the binomial test at which $H_0^{(1)}$ is rejected, and the eighth the significance level ($\alpha^{(2)}$) of the Wilcoxon test at which $H_0^{(2)}$ is rejected. We report in bold the case where both tests are rejected at a 0.01 significance level.

Dataset	N_{tot}	α
ν	349	0.26
$\dot{\nu}$	**349**	**0.02**

Table 3: Results of the test of hypothesis $H_0^{(3)}$. The first column reports the dataset used, the second the total number of data (N_{tot}), and the third the significance level ($\alpha^{(3)}$) of the Wilcoxon test at which $H_0^{(3)}$ is rejected. We report in bold the case where the test is rejected at a 0.05 significance level.

Region ID	Region Name	"preferred"	conjugate
3	BERING SEA	+	+
5	NEAR ISLANDS, ALEUTIAN ISLANDS	-	-
6	RAT ISLANDS, ALEUTIAN ISLANDS	-	+
7	ANDREANOF ISLANDS, ALEUTIAN IS.	+	-
9	FOX ISLANDS, ALEUTIAN ISLANDS	-	+
12	ALASKA PENINSULA	-	+
165	NORTH OF MACQUARIE ISLAND	-	+
166	AUCKLAND ISLANDS, N.Z. REGION	+	-
167	MACQUARIE ISLAND REGION	-	-
171	SOUTH OF FIJI ISLANDS	-	-
174	TONGA ISLANDS REGION	-	-
175	SOUTH OF TONGA ISLANDS	-	+
176	NORTH OF NEW ZEALAND	-	-
178	KERMADEC ISLANDS, NEW ZEALAND	+	-
179	SOUTH OF KERMADEC ISLANDS	-	+
181	FIJI ISLANDS REGION	-	-
182	FIJI ISLANDS	-	-
183	SANTA CRUZ ISLANDS REGION	-	-
184	SANTA CRUZ ISLANDS	+	-
185	VANUATU ISLANDS REGION	-	-
186	VANUATU ISLANDS	-	+
188	LOYALTY ISLANDS	+	-
189	SOUTHEAST OF LOYALTY ISLANDS	-	-
190	NEW IRELAND REGION, P.N.G.	-	+

Region ID	Region Name	"preferred"	conjugate
192	NEW BRITAIN REGION, P.N.G.	+	-
193	SOLOMON ISLANDS	+	-
196	IRIAN JAYA REGION, INDONESIA	-	+
197	NEAR NORTH COAST OF IRIAN JAYA	-	+
199	ADMIRALTY ISLANDS REGION, P.N.G.	-	-
200	NEAR N COAST OF NEW GUINEA, PNG.	-	+
202	NEW GUINEA, PAPUA NEW GUINEA	+	-
203	BISMARCK SEA	-	-
204	ARU ISLANDS REGION, INDONESIA	-	-
211	SOUTHEAST OF HONSHU, JAPAN	-	-
212	BONIN ISLANDS, JAPAN REGION	-	-
215	MARIANA ISLANDS REGION	-	-
216	MARIANA ISLANDS	-	-
218	NEAR EAST COAST OF KAMCHATKA	+	-
219	OFF EAST COAST OF KAMCHATKA	+	-
220	NORTHWEST OF KURIL ISLANDS	-	+
221	KURIL ISLANDS	-	+
222	EAST OF KURIL ISLANDS	-	-
223	EASTERN SEA OF JAPAN	-	-
224	HOKKAIDO, JAPAN REGION	+	-
225	OFF COAST OF HOKKAIDO, JAPAN	-	+
226	NEAR WEST COAST OF HONSHU, JAPAN	+	-
227	EASTERN HONSHU, JAPAN	-	-
228	NEAR EAST COAST OF HONSHU, JAPAN	-	+

Region ID	Region Name	"preferred"	conjugate
229	OFF EAST COAST OF HONSHU, JAPAN	+	-
230	NEAR S. COAST OF HONSHU, JAPAN	-	-
232	WESTERN HONSHU, JAPAN	-	-
233	NEAR S. COAST OF WESTERN HONSHU	-	-
234	NORTHWEST OF RYUKYU ISLANDS	-	+
235	KYUSHU, JAPAN	-	+
237	SOUTHEAST OF SHIKOKU, JAPAN	-	-
238	RYUKYU ISLANDS, JAPAN	-	-
240	WEST OF BONIN ISLANDS	-	-
243	TAIWAN REGION	-	-
244	TAIWAN	-	+
247	SOUTHEAST OF TAIWAN	-	+
248	PHILIPPINE ISLANDS REGION	+	+
249	LUZON, PHILIPPINES	+	-
251	SAMAR, PHILIPPINES	+	-
254	PANAY, PHILIPPINES	+	-
255	CEBU, PHILIPPINES	+	+
259	MINDANAO, PHILIPPINES	-	-
262	CELEBES SEA	-	+
263	TALAUD ISLANDS, INDONESIA	+	-
265	MINAHASSA PENINSULA, SULAWESI	-	+
266	NORTHERN MOLUCCA SEA	+	-
272	SERAM, INDONESIA	+	-
273	SOUTHWEST OF SUMATRA, INDONESIA	+	+

Region ID	Region Name	"preferred"	conjugate
274	SOUTHERN SUMATRA, INDONESIA	-	+
275	JAVA SEA	+	+
276	SUNDA STRAIT, INDONESIA	-	+
278	BALI SEA	+	+
279	FLORES SEA	+	+
280	BANDA SEA	-	-
281	TANIMBAR ISLANDS REG., INDONESIA	-	-
282	SOUTH OF JAVA, INDONESIA	-	+
283	BALI REGION, INDONESIA	-	+
284	SOUTH OF BALI, INDONESIA	+	+
285	SUMBAWA REGION, INDONESIA	-	-
286	FLORES REGION, INDONESIA	-	+
287	SUMBA REGION, INDONESIA	+	+
289	TIMOR REGION	-	-
291	SOUTH OF SUMBAWA, INDONESIA	+	+
292	SOUTH OF SUMBA, INDONESIA	+	+
294	MYANMAR-INDIA BORDER REGION	-	+
297	MYANMAR-CHINA BORDER REGION	+	+
305	WESTERN XIZANG-INDIA BORDER REG.	+	-
306	XIZANG	+	+
308	NORTHERN INDIA	-	+
309	NEPAL-INDIA BORDER REGION	+	+
310	NEPAL	-	+

Region ID	Region Name	"preferred"	conjugate
311	SIKKIM, INDIA	+	+
314	SOUTHERN INDIA	+	-
318	YUNNAN, CHINA	+	+
320	KYRGYZSTAN-XINJIANG BORDER REG.	+	+
321	SOUTHERN XINJIANG, CHINA	-	+
325	QINGHAI, CHINA	+	+
326	SOUTHWESTERN SIBERIA, RUSSIA	-	-
328	EAST OF LAKE BAYKAL, RUSSIA	-	-
330	LAKE ISSYK-KUL REGION	-	-
333	RUSSIA-MONGOLIA BORDER REGION	-	-
337	EASTERN CAUCASUS	-	-
338	CASPIAN SEA	-	-
339	NORTHWESTERN UZBEKISTAN	+	-
340	TURKMENISTAN	-	-
341	TURKMENISTAN-IRAN BORDER REGION	-	-
344	ARMENIA-AZERBAIJAN-IRAN BORD REG	-	+
345	NORTHWESTERN IRAN	+	-
346	IRAN-IRAQ BORDER REGION	-	-
347	WESTERN IRAN	-	-
358	ROMANIA	+	-
362	NORTHWESTERN CAUCASUS	+	-
365	AEGEAN SEA	-	-
366	TURKEY	-	-
368	SOUTHERN GREECE	+	-

Region ID	Region Name	"preferred"	conjugate
369	DODECANESE ISLANDS, GREECE	-	-
370	CRETE, GREECE	-	-
383	NORTHWESTERN BALKAN REGION	+	-
390	SOUTHERN ITALY	-	-
392	GREECE-ALBANIA BORDER REGION	-	-
396	NORTHERN ALGERIA	+	-
398	SICILY, ITALY	-	-
399	IONIAN SEA	-	-
400	CENTRAL MEDITERRANEAN SEA	+	-
420	NORTH INDIAN OCEAN	+	+
426	CHAGOS ARCHIPELAGO REGION	+	+
427	MAURITIUS - REUNION REGION	-	-
429	MID-INDIAN RIDGE	-	+
431	PRINCE EDWARD ISLANDS REGION	+	+
435	SOUTHEAST INDIAN RIDGE	-	-
553	EGYPT	-	-
554	RED SEA	-	-
555	WESTERN ARABIAN PENINSULA	-	-
558	ETHIOPIA	+	+
567	DEMOCRATIC REPUBLIC OF CONGO	+	-
568	UGANDA	-	-
572	LAKE TANGANYIKA REGION	-	-
574	NORTHWEST OF MADAGASCAR	-	-
577	MALAWI	-	-

Region ID	Region Name	"preferred"	conjugate
588	NORTHWEST OF AUSTRALIA	-	+
590	WESTERN AUSTRALIA	-	-
591	NORTHERN TERRITORY, AUSTRALIA	+	+
638	ICELAND	-	-
640	GREENLAND SEA	-	-
655	LAPTEV SEA	-	-
656	SOUTHEASTERN SIBERIA, RUSSIA	-	-
657	E. RUSSIA-N.E. CHINA BORDER REG.	-	+
658	NORTHEASTERN CHINA	-	+
659	NORTH KOREA	-	+
661	PRIMOR'YE, RUSSIA	-	-
663	SEA OF OKHOTSK	-	-
670	NEAR N. COAST OF EASTERN SIBERIA	-	-
671	EASTERN SIBERIA, RUSSIA	+	-
676	NORTHERN ALASKA	-	-
688	EAST OF NORTH ISLAND, N.Z.	+	-
701	WEST OF MACQUARIE ISLAND	+	+
704	NICOBAR ISLANDS, INDIA REGION	+	+
705	OFF W COAST OF NORTHERN SUMATRA	-	-
706	NORTHERN SUMATRA, INDONESIA	+	+
710	PAKISTAN	+	-
716	KYRGYZSTAN	+	-
717	AFGHANISTAN-TAJIKISTAN BORD REG.	+	+
718	HINDU KUSH REGION, AFGHANISTAN	+	-

Region ID	Region Name	"preferred"	conjugate
720	NORTHWESTERN KASHMIR	-	-
736	VIETNAM	+	+
740	OWEN FRACTURE ZONE REGION	-	-
742	WESTERN INDIAN-ANTARCTIC RIDGE	+	+

Table 4: Database for the forward test. See text for more details.

Figure captions

Figure 1: Plot of the earthquakes seismic moment reported in the Pacheco and Sykes' catalog (1992) as a function of their occurrence time. The black, blue, red, and green colors identify, respectively, the events not considered into the analysis, the events occurred "before" the giant events, the period when the giants events occurred, and the events occurred "after" the giant events. The horizontal dotted line represents the energy released by the Sumatra-Andaman (2004-2005) earthquakes.

Figure 2: Plot of the sign of $\dot{\nu}$ (red positive, blue negative) calculated at each epicentral location of earthquakes occurred in period I (upper panel), and in period II (lower panel).

Figure 3: Plot of the variable Δ (see text for more details). Black dots represent the location of source earthquakes.

Figure 4: Forecast of the effect of recent Sumatra-Andaman earthquakes on the worldwide seismicity, using a) preferred focal mechanisms, b) conjugate focal mechanisms, c) areas where there is agreement on the sign of perturbations on both focal mechanisms (see text for more details). Red/blue areas experience positive/negative perturbations.

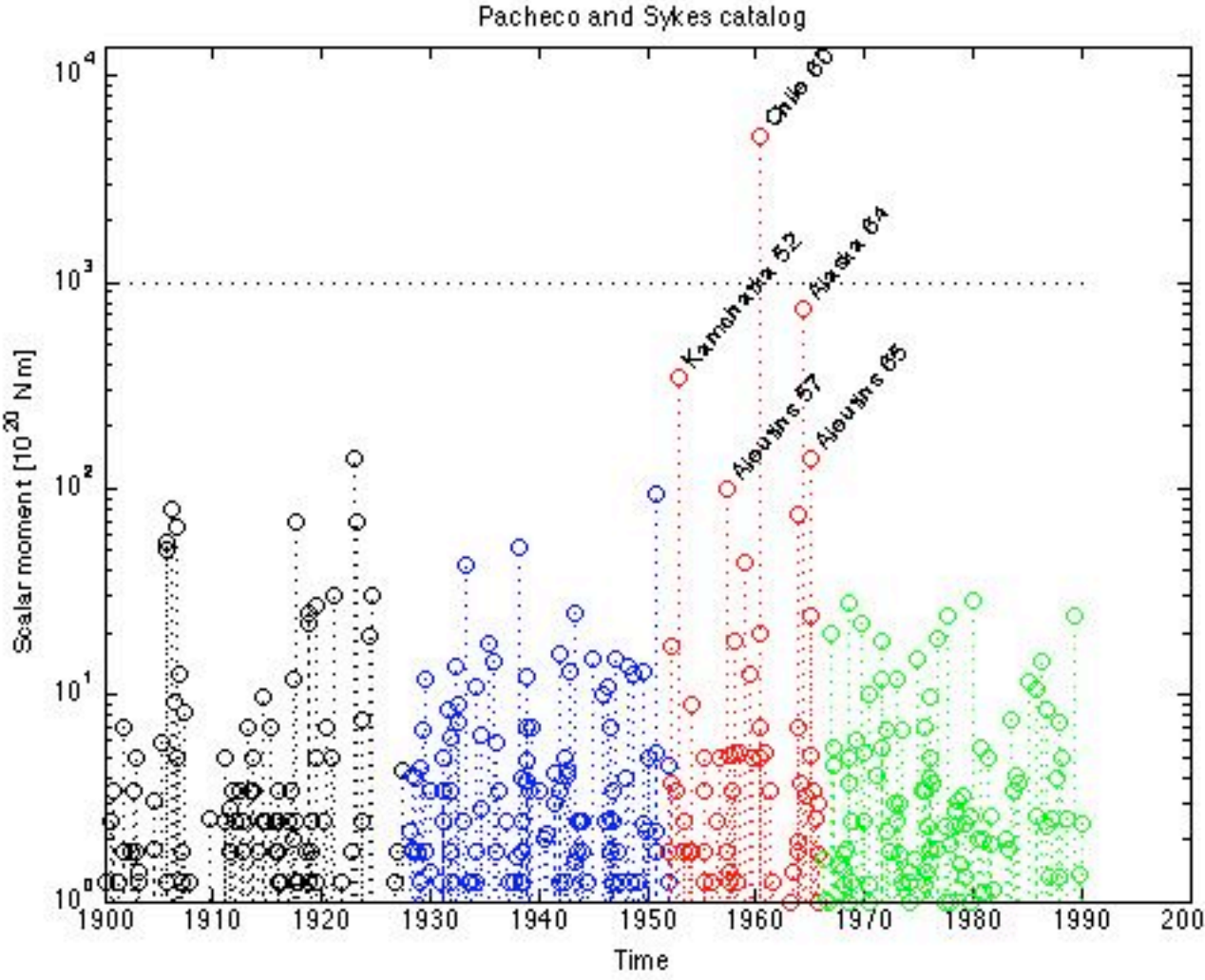
Pacheco and Sykes catalog
Scalar moment [10^20 N m]
Time
Chile 60
Kamchatka 52
Alaska 64
Aleutians 57
Aleutians 65

PERIOD 1928-1951

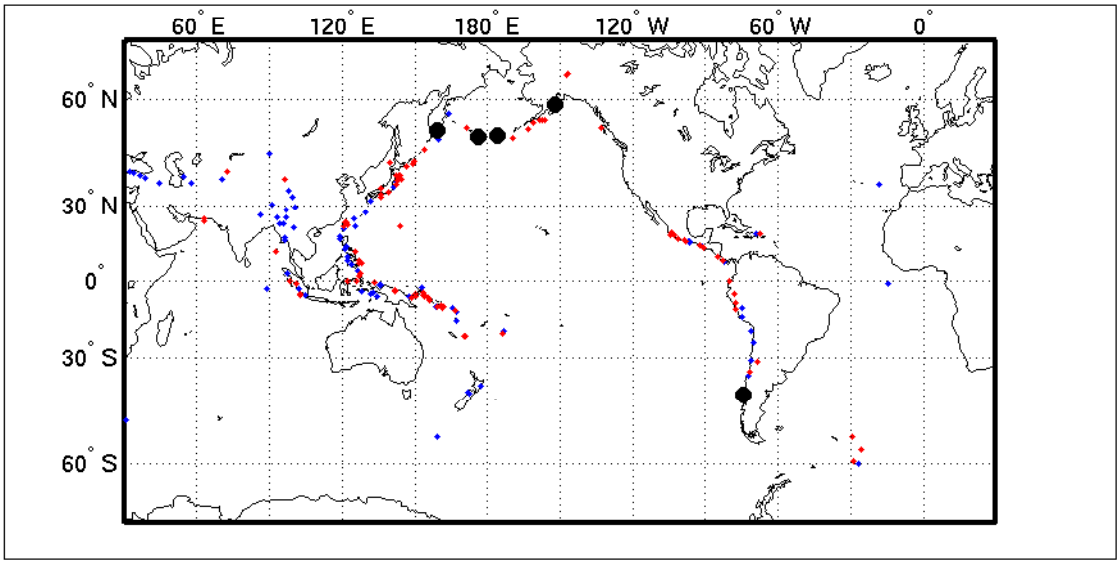

PERIOD 1966-1989

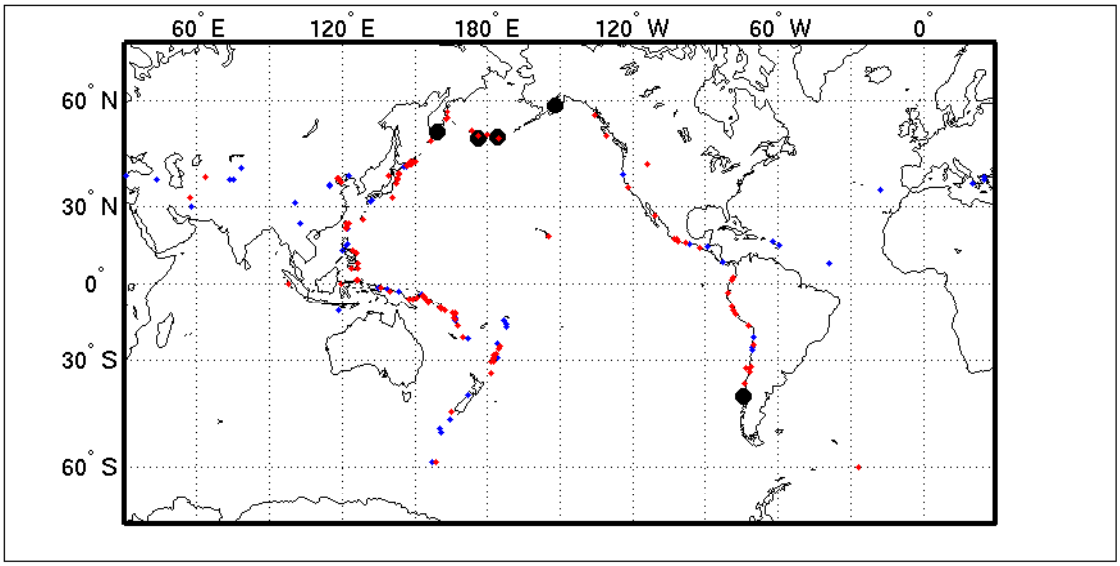

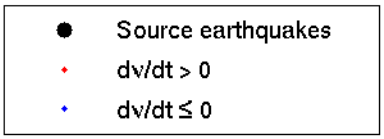

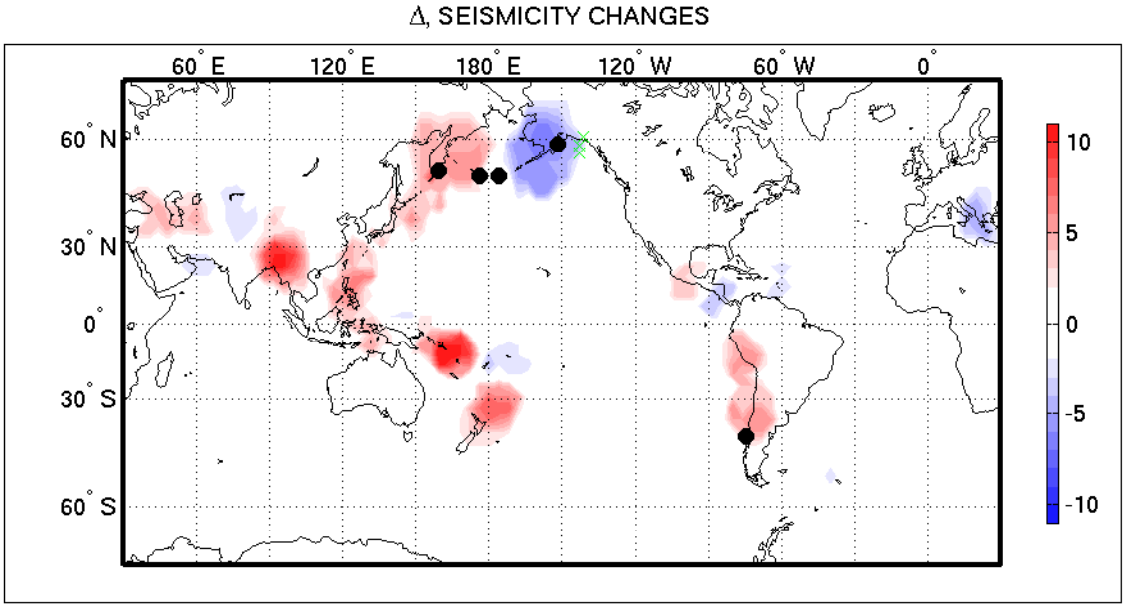
Δ, SEISMICITY CHANGES
60° E
120° E
180° E
120° W
60° W
0°
60° N
30° N
0°
30° S
60° S
10
5
0
-5
-10

PREFERRED FOCAL MECHANISMS

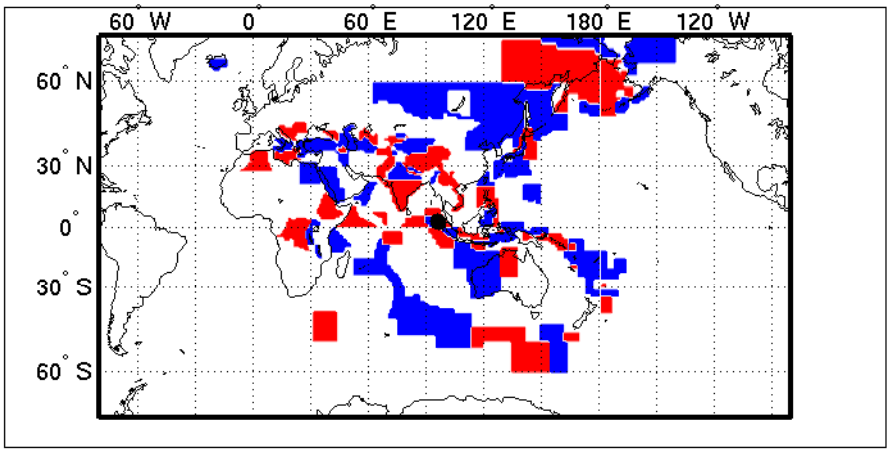

CONJUGATE FOCAL MECHANISMS

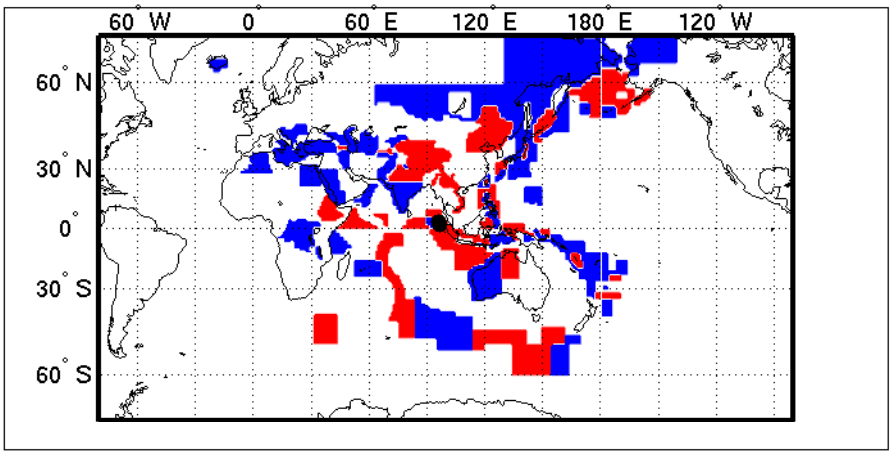

COHERENT FOCAL MECHANISMS